

ELECTRONIC SUPPLEMENTARY INFORMATION

Polymer Assisted Synthesis of Chain-like Cobalt-Nickel Alloy Nanostructures:

Magnetically Recoverable and Reusable Catalysts with High Activities

Md. Harunar Rashid, Manoj Raula, and Tarun K. Mandal*

Polymer Science Unit, Indian Association for the Cultivation of Science, Jadavpur, Kolkata 700 032, India

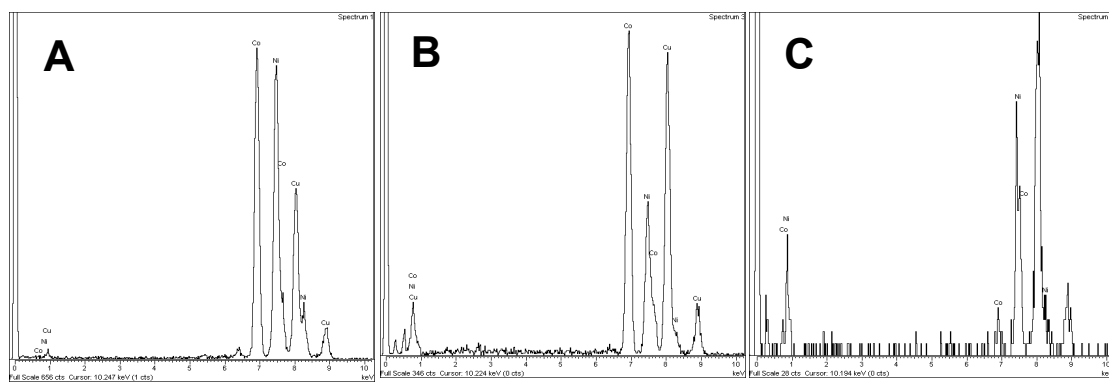


Figure S1. EDX spectra of different CoNi alloy samples: (A) PCo₁Ni₁; (B) PCo₂Ni₁ and (C) PCo₁Ni₂

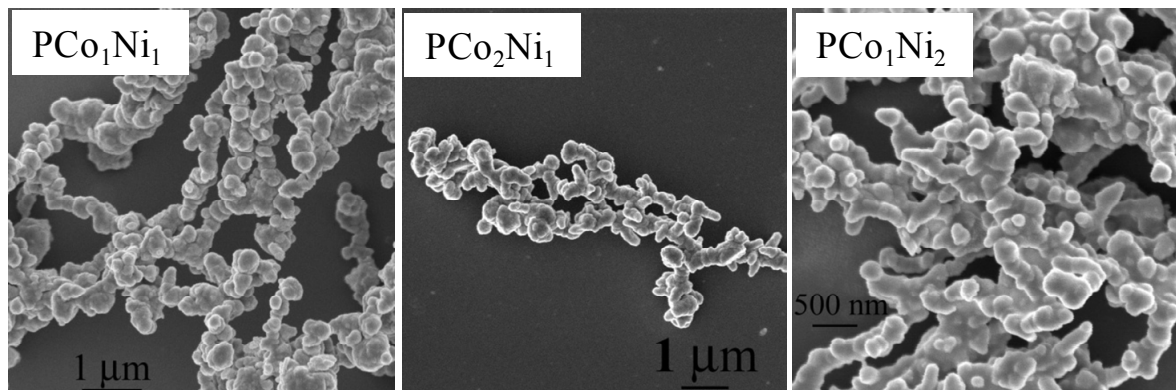


Figure S2. Field emission scanning electron micrographs of different alloy samples showing their chainlike structures.

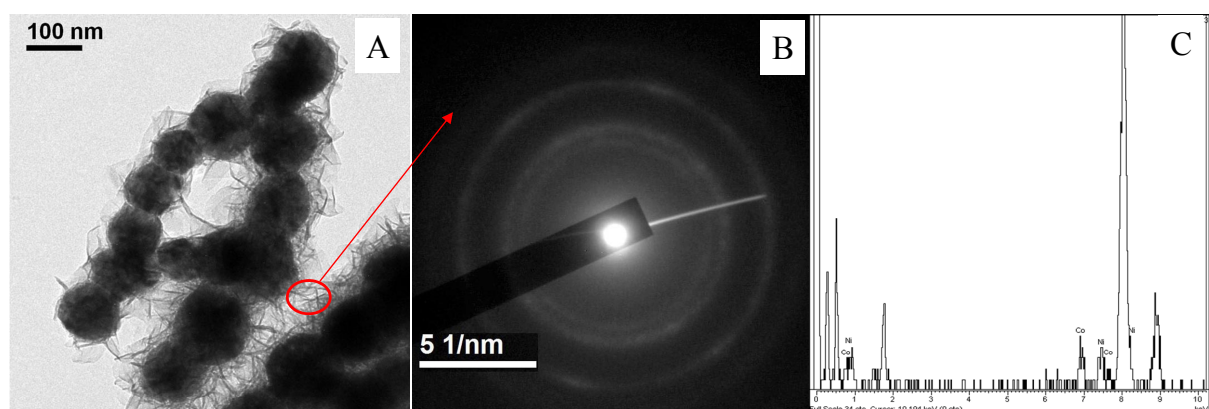


Figure S3. (A) TEM images of the samples PCo₁Ni₁ (B) The NBD patterns of the marked portion of the alloy nanostructures given in the left panel (C) EDX patterns taken from the specified portion of Figure A.

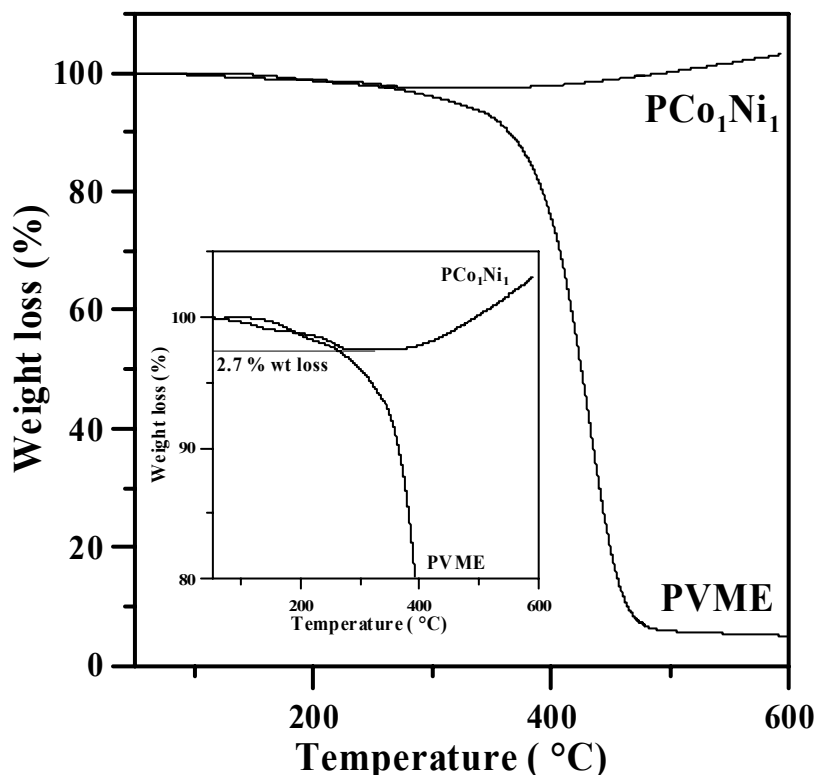


Figure S4. TGA thermogram of the sample PCo₁Ni₁ and neat polymer PVME. A magnified portion of the graph is given in the inset. TGA thermograms show that only 2.7 wt % is adsorbed on the surface of the alloy nanostructures.

The thermogram of PVME-coated CoNi nanocomposites (PCo₁Ni₁) is shown in Figure S3 along with the TGA thermogram of neat PVME for comparison. From the TGA it is found that only around 2.7 wt% loses during the experiment (see inset of Figure S3 in the SI). Neat PVME starts decomposing at ~ 310 °C. The significant weight loss, registered in case of neat PVME was ~ 90 % between 150 and 490 °C. But, for the nanocomposites, a significant weight loss of 2.7 % was registered upto 280 °C and became stable upto 370 °C. This weight loss is attributable to the surface adsorbed PVME and acetylacetone group present at the surface of CoNi alloys as confirmed from the FT-IR results (see Figure 4). Beyond this temperature, the curve increases sharply and a considerable amount of weight gain (5.5 %/ 3% compared to the initial amount) was noticed. We expect that as the surface adsorbed PVME was burnt out, the alloy powders began to be oxidized at around 370 °C, receiving a weight gain.

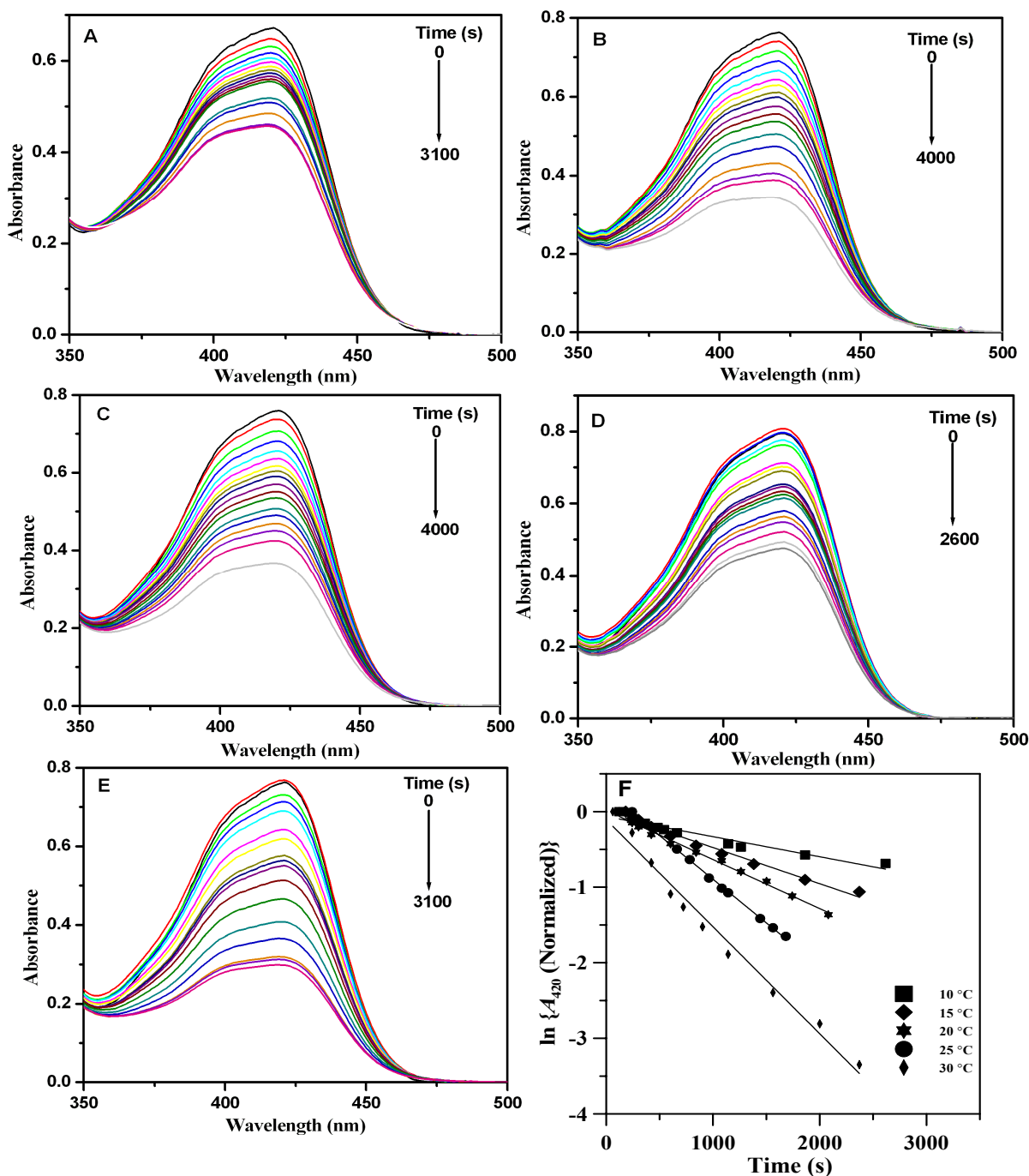


Figure S5. Successive UV-Vis spectra of $\text{K}_3[\text{Fe}(\text{CN})_6]$ during its reaction with $\text{Na}_2\text{S}_2\text{O}_3$ in presence of PCo_1Ni_1 catalyzed at differ temperatures such as: (A) 10 °C; (B) 15 °C; (C) 20 °C; (D) 25 °C and (E) 30 °C. (F) Plots of $\ln A_{420}$ vs. time at these temperatures.

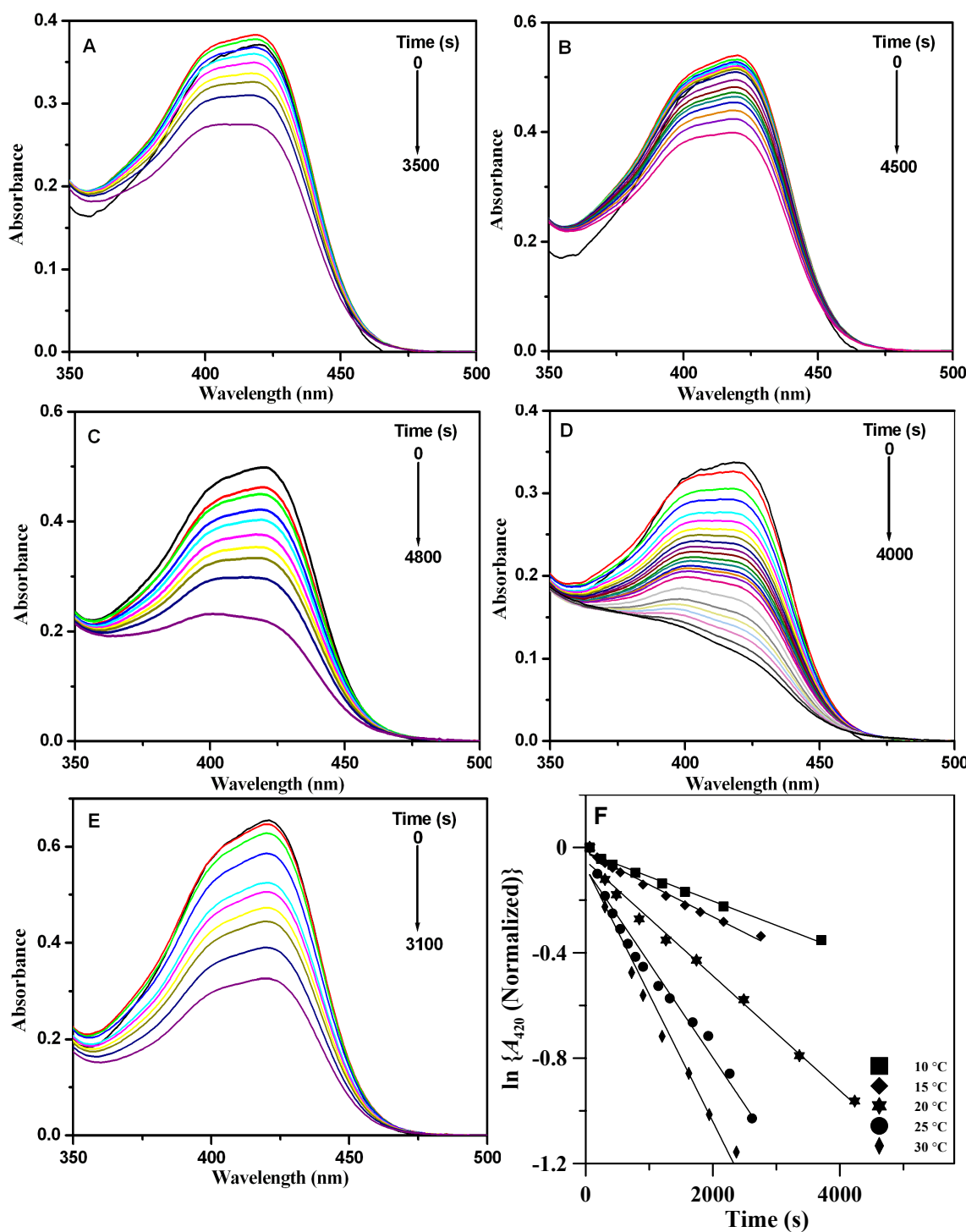


Figure S6. Successive UV-Vis spectra of $\text{K}_3[\text{Fe}(\text{CN})_6]$ during its reaction with $\text{Na}_2\text{S}_2\text{O}_3$ in presence of PCo_2Ni_1 catalyzed at differ temperatures such as: (A) 10 °C; (B) 15 °C; (C) 20 °C; (D) 25 °C and (E) 30 °C. (F) Plots of $\ln A_{420}$ vs. time at these temperatures.

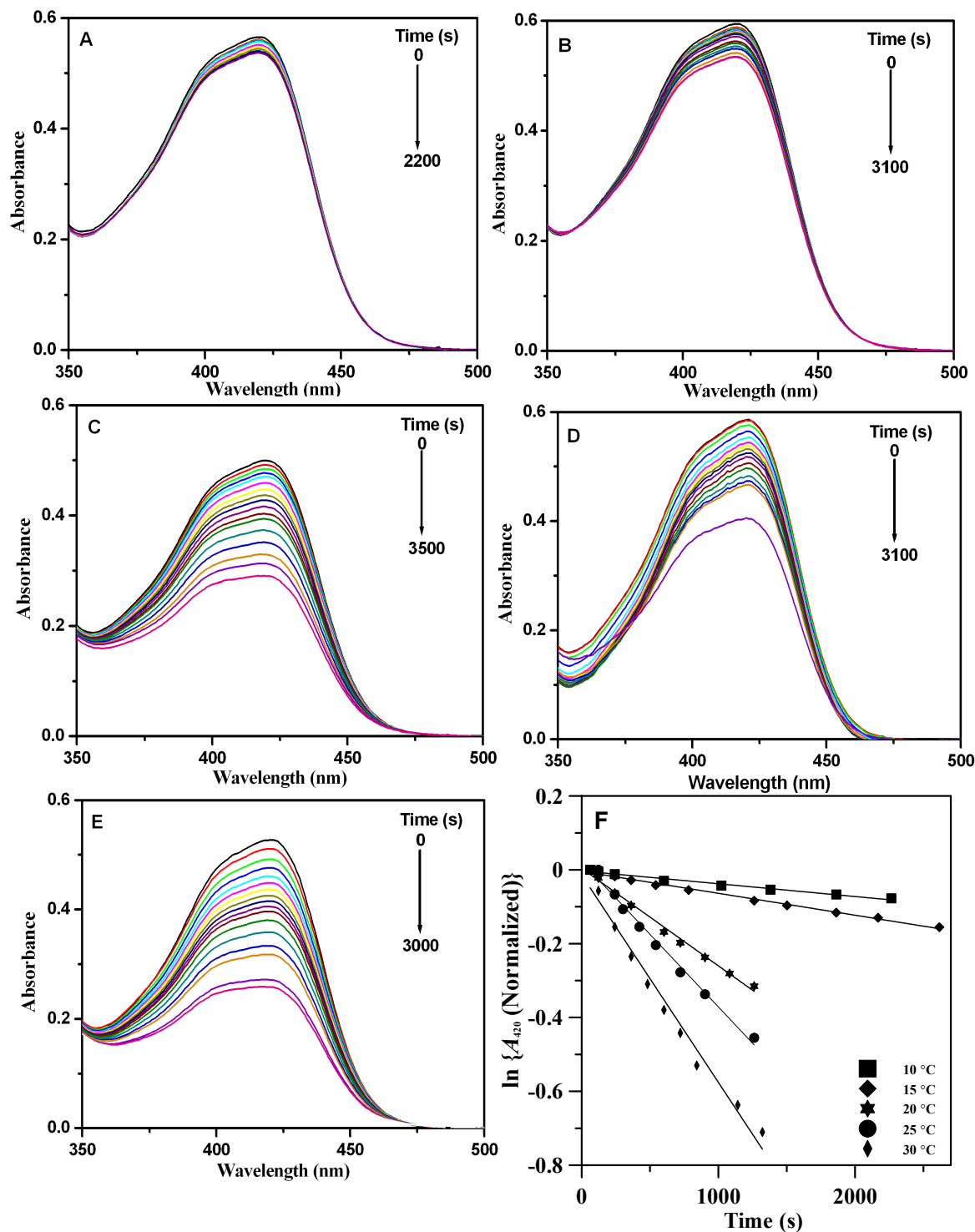


Figure S7. Successive UV-Vis spectra of $\text{K}_3[\text{Fe}(\text{CN})_6]$ during its reaction with $\text{Na}_2\text{S}_2\text{O}_3$ in presence of PCo_1Ni_2 catalyzed at different temperatures such as: (A) 10 °C; (B) 15 °C; (C) 20 °C; (D) 25 °C and (E) 30 °C. (F) Plots of $\ln A_{420}$ vs. time at these temperatures.

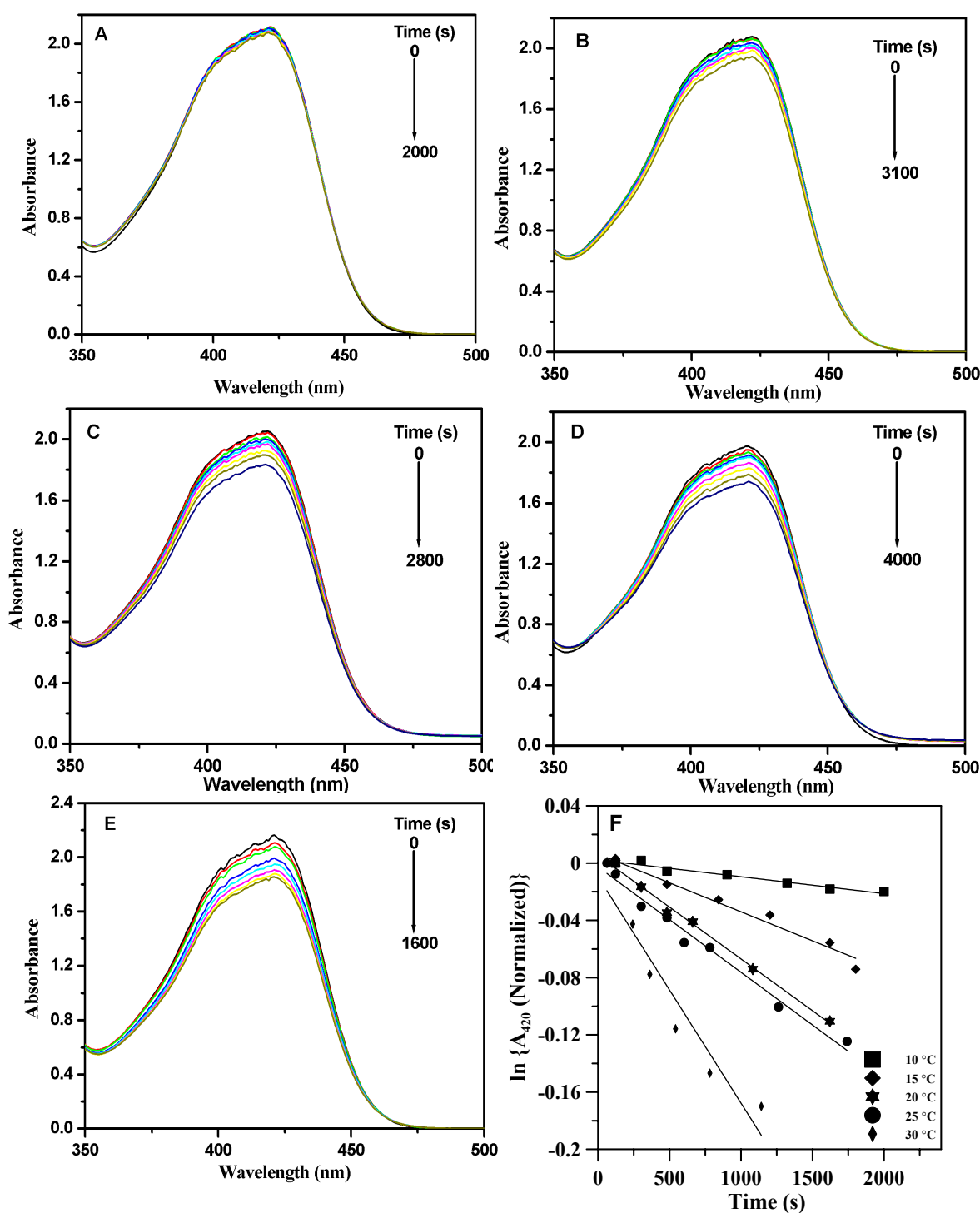


Figure S8. Successive UV-Vis spectra of $\text{K}_3[\text{Fe}(\text{CN})_6]$ during its reaction with $\text{Na}_2\text{S}_2\text{O}_3$ in presence of Co_1Ni_1 catalyzed at differ temperatures such as: (A) 10 °C; (B) 15 °C; (C) 20 °C; (D) 25 °C and (E) 30 °C. (F) Plots of $\ln A_{420}$ vs. time at these temperatures.

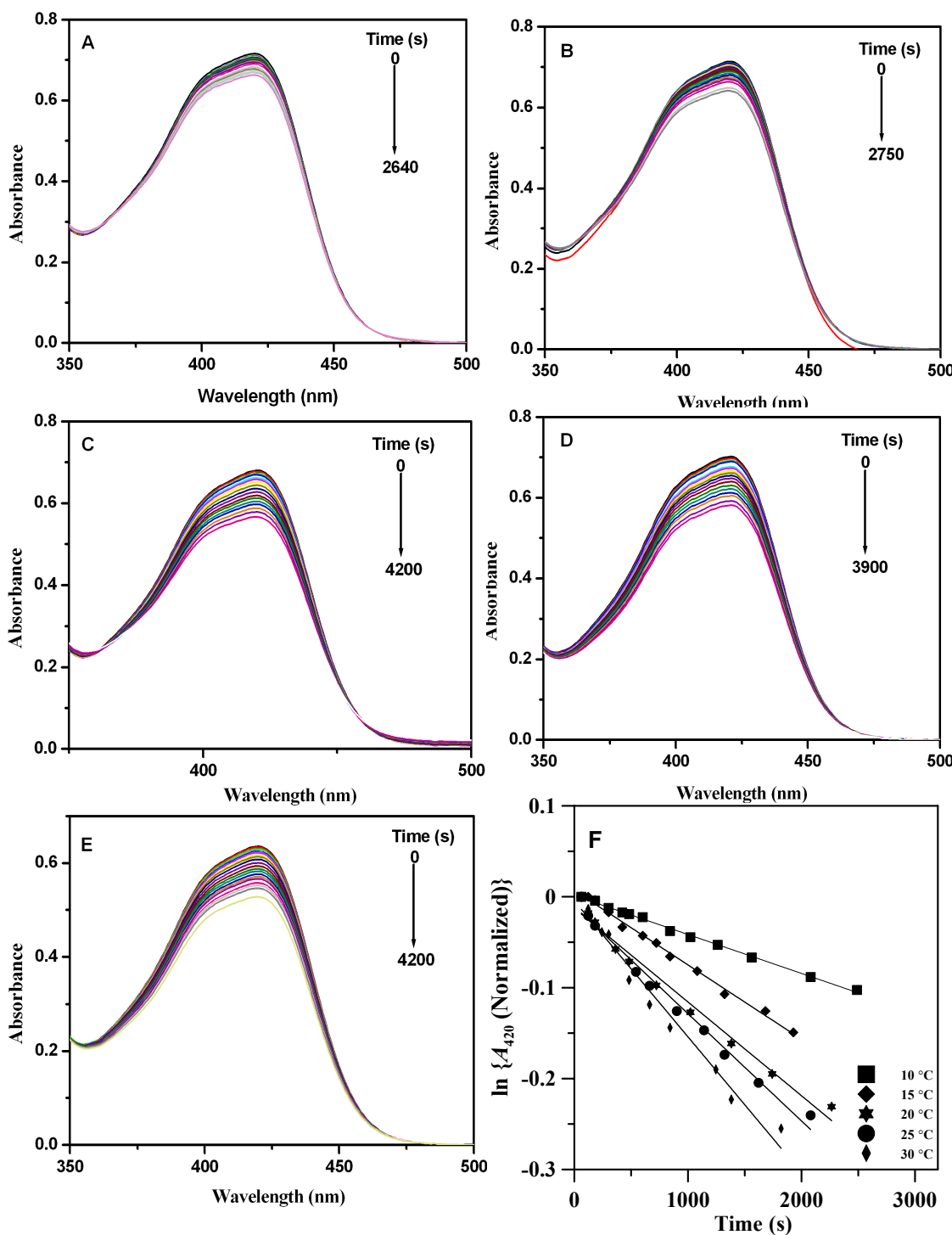


Figure S9. Successive UV-Vis spectra of $\text{K}_3[\text{Fe}(\text{CN})_6]$ during its reaction with $\text{Na}_2\text{S}_2\text{O}_3$ in presence of PCo catalyzed at differ temperatures such as: (A) 10 °C; (B) 15 °C; (C) 20 °C; (D) 25 °C and (E) 30 °C. (F) Plots of $\ln A_{420}$ vs. time at these temperatures.

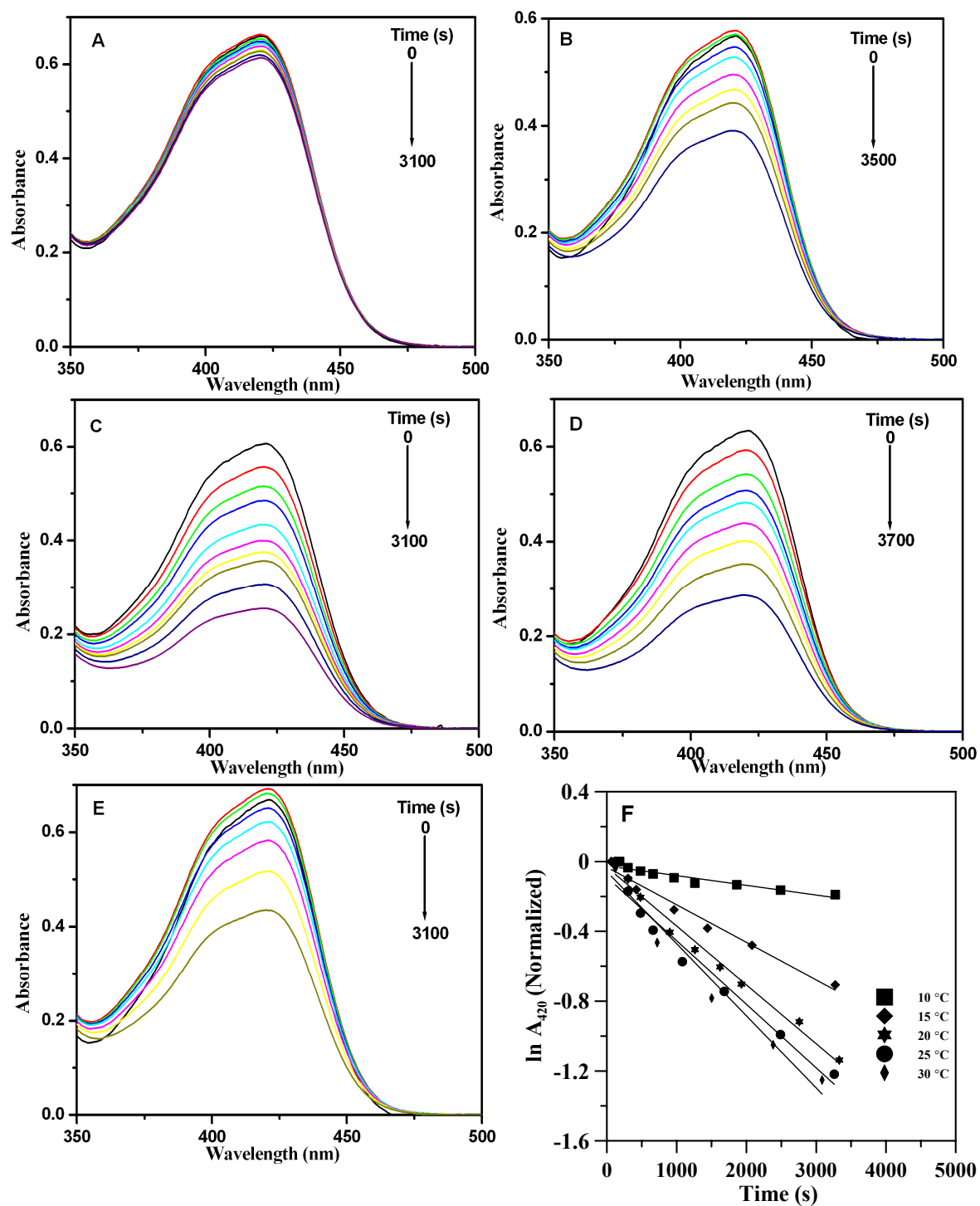


Figure S10. Successive UV-Vis spectra of $K_3[Fe(CN)_6]$ during its reaction with $Na_2S_2O_3$ in presence of PNi catalyzed at differ temperatures such as: (A) 10 °C; (B) 15 °C; (C) 20 °C; (D) 25 °C and (E) 30 °C. (F) Plots of $\ln A_{420}$ vs. time at these temperatures.

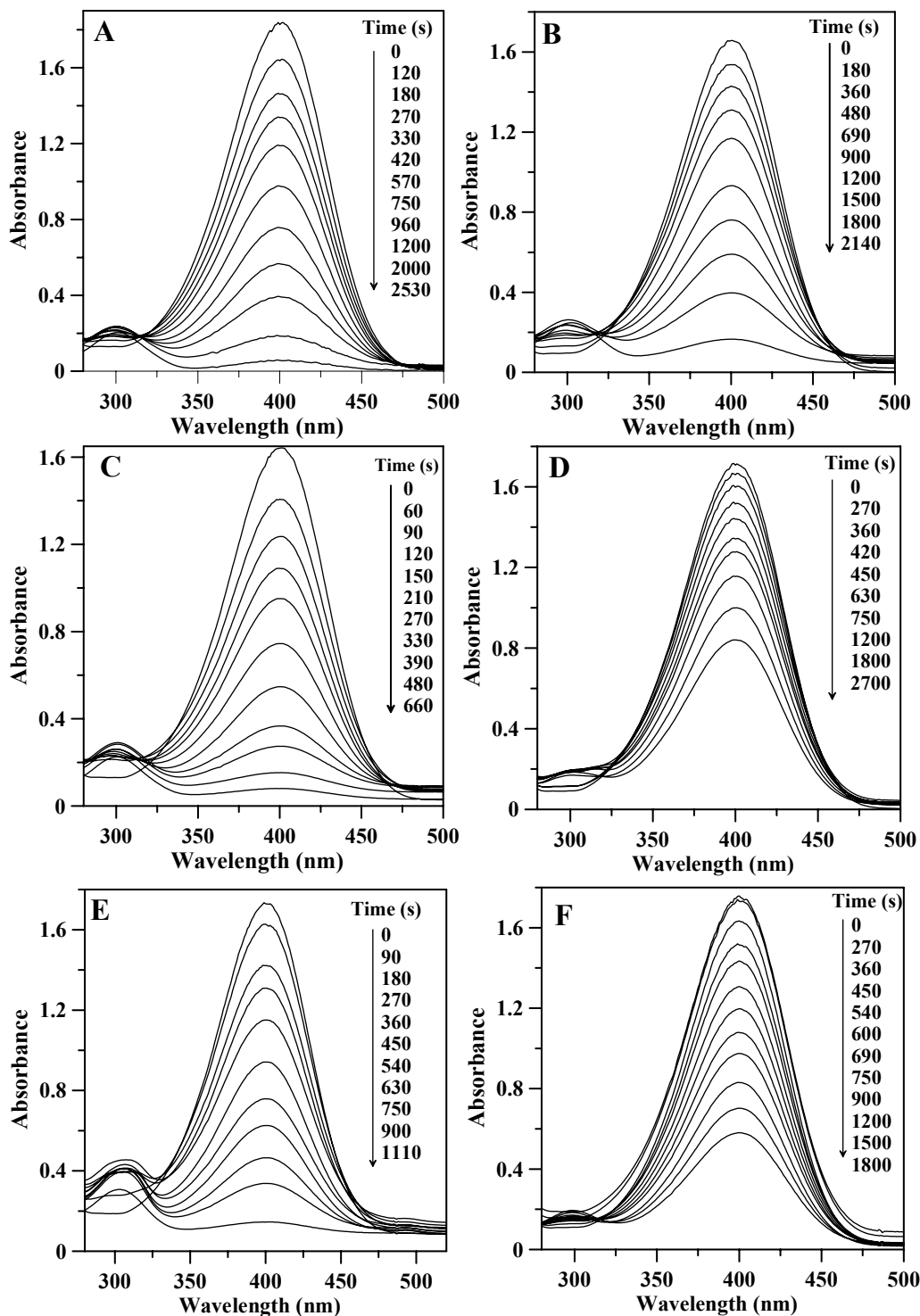


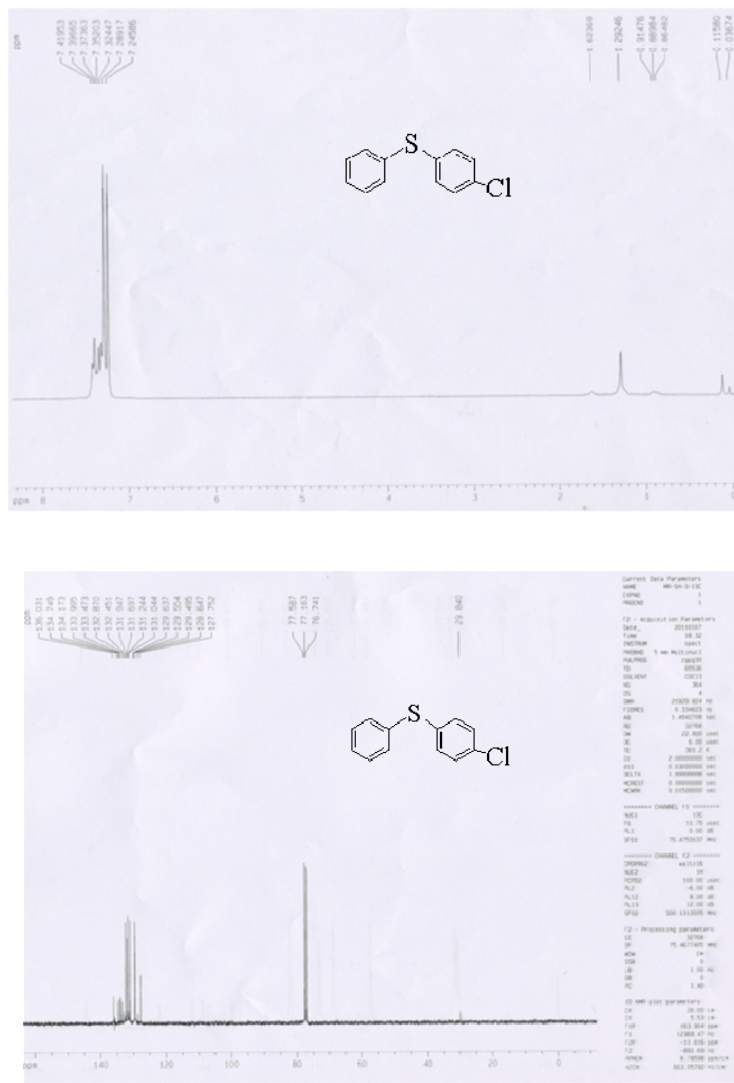
Figure S11. Plot showed the variation of absorbance with wavelength at different time for the reduction of *p*-nitrophenol with NaBH₄ for the different sample of Co-Ni nanostructures at 25 °C, (A) PCo₁Ni₁; (B) PCo₂Ni₁; (C) PCo₁Ni₂; (D) Co₁Ni₁; (E) PCo; (F) PNi.

4-Chlorodiphenyl sulfide

Colorless oil; ^1H NMR(300 MHz, CDCl₃) 7.25-7.38(9H, m).

^{13}C NMR (75 MHz, CDCl₃) 127.54, 129.28, 129.61, 131.17, 131.43, 132.89

Reference: Y.-J. Chen and H.-H. Chen, *Org. Lett.*, 2006, **8**, 5609-5612.



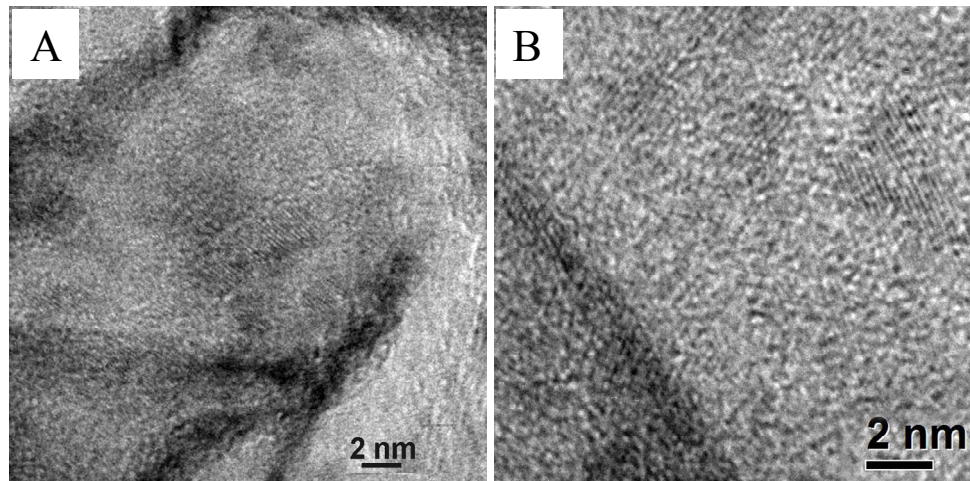


Figure S13. HRTEM images of the amorphous shell of PCo_1Ni_1 nanochain catalyst: (A) before the borohydride reduction of p-nitrophenol and (B) after the borohydride reduction of p-nitrophenol.